# Dissecting the impact of $CO_2$ and pH on the mechanisms of photosynthesis and calcification in the coccolithophore *Emiliania huxleyi*

Lennart T. Bach[1,*], Luke C. M. Mackinder[1,2,4,*], Kai G. Schulz[1], Glen Wheeler[2,3], Declan C. Schroeder[2], Colin Brownlee[2] and Ulf Riebesell[1]

1Helmholtz-Zentrum für Ozeanforschung Kiel (GEOMAR), D24105, Kiel, Germany; 2Marine Biological Association of the UK, The Laboratory, Citadel Hill, Plymouth, PL1 2PB, UK; 3Plymouth Marine Laboratory, Prospect Place, Plymouth, PL1 3DH, UK; 4 Present address: Department of Plant Biology, Carnegie Institution, 260 Panama Street, Stanford, CA 94305, USA

*These authors contributed equally to this work.

## Summary

- Coccolithophores are important calcifying phytoplankton predicted to be impacted by changes in ocean carbonate chemistry caused by the absorption of anthropogenic $CO_2$. However, it is difficult to disentangle the effects of the simultaneously changing carbonate system parameters ($CO_2$, bicarbonate, carbonate and protons) on the physiological responses to elevated $CO_2$.
- Here, we adopted a multifactorial approach at constant pH or $CO_2$ whilst varying dissolved inorganic carbon (DIC) to determine physiological and transcriptional responses to individual carbonate system parameters.
- We show that *Emiliania huxleyi* is sensitive to low $CO_2$ (growth and photosynthesis) and low bicarbonate (calcification) as well as low pH beyond a limited tolerance range, but is much less sensitive to elevated $CO_2$ and bicarbonate. Multiple up-regulated genes at low DIC bear the hallmarks of a carbon-concentrating mechanism (CCM) that is responsive to $CO_2$ and bicarbonate but not to pH.
- *Emiliania huxleyi* appears to have evolved mechanisms to respond to limiting rather than elevated $CO_2$. Calcification does not function as a CCM, but is inhibited at low DIC to allow the redistribution of DIC from calcification to photosynthesis. The presented data provides a significant step in understanding how *E. huxleyi* will respond to changing carbonate chemistry at a cellular level.

## Introduction

Marine photoautotrophic organisms fix c. 55 gigatonnes of carbon $yr^{-1}$ which is equal to the photosynthetic production by the terrestrial biosphere (Field et al., 1998). Coccolithophores play a major role in the global carbon cycle by contributing c. 1–10% to total organic carbon fixation (Poulton et al., 2007) and providing ballast through the formation of calcite, which enhances organic matter sinking into the deep ocean (Thierstein et al., 1977). The globally most abundant coccolithophore species is *Emiliania huxleyi*, which has the ability to form blooms up to $8 \times 10^6$ $km^2$ (Moore et al., 2012). Despite the global significance of *E. huxleyi*, there is only a limited understanding of important cellular processes and their response to environmental change.

Under present-day conditions, marine phytoplankton growth is mostly limited by low light availability or by the insufficient supply of inorganic nutrients, such as nitrogen, phosphorus or iron (Sarmiento & Gruber, 2006), while carbon dioxide ($CO_2$) is usually not considered to be limiting. Nevertheless, $CO_2$ diffusion rates are in most cases not high enough to account

for the photosynthetic rates seen in the majority of phytoplankton (Falkowski & Raven, 2007). This discrepancy is explained by the action of carbon (or $CO_2$) concentrating mechanisms (CCMs). In algae these are predominantly C3 biophysical mechanisms which link carbonic anhydrases (CAs), dissolved inorganic carbon (DIC) transporters and pH gradients to enhance [$CO_2$] at the active site of Ribulose-1,5-bisphosphate carboxylase oxygenase (RubisCO) (Reinfelder, 2011). It is thought that nearly all marine phytoplankton operate a CCM, although the DIC species used ($CO_2$ and/or bicarbonate ($HCO_3^-$)), its regulation, cellular components, and DIC affinity can vary significantly between species (Giordano et al., 2005). *E. huxleyi* operates a low-affinity CCM (Rost et al., 2003). Several studies indicate that $CO_2$ is the primary source for photosynthesis, although there are some discrepancies over the importance of $HCO_3^-$, especially at lower $CO_2$ concentrations (Paasche, 1964; Sikes et al., 1980; Nimer & Merrett, 1992; Sekino & Shiraiwa, 1994; Herfort et al., 2002; Rost et al., 2003; Schulz et al., 2007; Bach et al., 2011). In addition to a biophysical mechanism, intracellular calcification has been proposed to act as a CCM by providing protons ($H^+$) as a by-product of calcification to support the dehydration of $HCO_3^-$ to $CO_2$ (reviewed in; Paasche, 2001). Although there are some supporting data (Nimer & Merrett, 1992; Buitenhuis et al., 1999), other studies contradict the concept (Paasche, 1964; Herfort et al., 2004; Trimborn et al., 2007; Leonardos et al., 2009).

In the forthcoming centuries, ongoing uptake of anthropogenic atmospheric $CO_2$ into the oceans will continuously change the marine carbonate chemistry – a process known as ocean acidification (Caldeira & Wickett, 2003). Chemically, ocean acidification leads to a strong decrease of the carbonate ion ($CO_2^-{}_3$) concentration, a slight increase in [$HCO_3^-$] and a strong increase in [$CO_2$] and [$H^+$] (Wolf-Gladrow et al., 1999). These components are thought to affect coccolithophores in varying ways, with [$CO_2^-{}_3$] influencing calcite saturation concentrations, [$H^+$] affecting cellular pH homeostasis, [$CO_2$] affecting photosynthesis and [$HCO_3^-$] influencing calcification (and photosynthesis). The potential effects of ocean acidification on calcification and photosynthesis by *E. huxleyi* have been repeatedly reported (reviewed in Riebesell & Tortell, 2011), but the importance of changes in the individual carbonate parameters for the observed responses is still not fully understood.

The present study disentangles the carbonate system to improve our conceptual understanding of the acquisition of DIC and its subsequent use in calcification and photosynthesis. In particular, we address two important questions in *E. huxleyi* ecophysiology: how sensitive is *E. huxleyi* to low and elevated components of the carbonate system; and does calcification act as a CCM?

## Materials and Methods

### Conceptual background of the experiments

The marine carbonate system is defined by the concentrations of $CO_2$, $HCO_3^-$, $CO_2^-{}_3$, $pCO_2$, total alkalinity (TA), DIC (i.e. combined $CO_2$, $HCO_3^-$ and $CO_2^-{}_3$), and pH ([$H^+$]; Zeebe & Wolf-Gladrow, 2001). The physiologically relevant parameters of the carbonate system are $CO_2$, $HCO_3^-$, $CO_2^-{}_3$ and $H^+$, as only these can be perceived by a cell. They are connected to each other in the equilibrium reaction:

$$CO_2 + H_2O \leftrightarrow HCO_3^- + H^+ \leftrightarrow CO_2^-{}_3 + 2H^+ \quad \text{Eqn 1}$$

As no other parameters of physiological relevance other than $CO_2$, $HCO_3^-$, $CO_2^-{}_3$ and $H^+$ were changed in the experiments (e.g. light or temperature), it is assumed that only changing concentrations of these particular parameters can induce physiological or genetic responses. $CO_2$, $HCO_3^-$, $CO_2^-{}_3$ and $H^+$ are closely codependent (Eqn 1) and any change in the concentration of one will lead to changes in the others. Nevertheless, it is possible to keep one of the four parameters constant while changing the other three. We made use of this feature and performed three experiments where we kept either [$CO_2$] or [$H^+$] constant between treatments ([$H^+$] was kept constant at two different concentrations). The constant carbonate system parameter within an experiment can be excluded from being responsible for the observed physiological or genetic response (Buitenhuis et al., 1999). Note that we chose to focus on $CO_2$ and $H^+$, as previous work points towards a primary importance of these particular parameters for *E. huxleyi* physiology (Schulz et al., 2007; Bach et al., 2011).

## Experimental design and basic setup

Three experiments were conducted to test the physiological and molecular responses of *Emiliania huxleyi* (Lohmann) Hay and Mohler to changes in individual carbonate chemistry parameters. DIC was varied in all experiments, while either $pH_f$ (8.34 or 7.74 on free scale) or $CO_2$ (16 µmol $kg^{-1}$) was kept constant. In all experiments, cells of *E. huxleyi* (strain B92/11) were grown in monoclonal dilute batch cultures (LaRoche et al., 2010) at 15°C and 150 µmol $m^{-2}$ $s^{-1}$ incident photon flux density under a 16:8h, light:dark cycle. The growth medium was artificial seawater prepared as described in Kester et al. (1967) but without the addition of $NaHCO_3$, which was added in a later step (see the following section). Artificial seawater was enriched with c. 64µmol $kg^{-1}$ nitrate, 4 µmol $kg^{-1}$ phosphate, f/8 concentrations of a trace metal and vitamin mixture (Guillard & Ryther, 1962), 10 nmol $kg^{-1}$ of $SeO_2$, and 2ml $kg^{-1}$ of natural North Sea water. Concentrations of nitrate and phosphate were measured according to Hansen & Koroleff (1999). The nutrient-enriched artificial seawater was sterile-filtered into polycarbonate bottles where the carbonate chemistry was manipulated. After taking samples for carbonate chemistry measurements (see the following section), the artificial seawater was divided carefully into three 2.3 l polycarbonate bottles before inoculation. Before inoculation, *E. huxleyi* cells were acclimated to exponential growth and carbonate chemistry conditions for at least seven generations. Approximate cell densities ranged from 50 to 300 cells $ml^{-1}$ at inoculation and 40 000–100 000 cells $ml^{-1}$ at sampling (see description of sampling later).

## Carbonate chemistry manipulation and determination

In all experiments, target DIC concentrations were adjusted by adding calculated amounts of $NaHCO_3$ or $Na_2CO_3$ (see Bach et al., 2012 for details). In the constant-$CO_2$ experiment, $CO_2$ was set to a constant concentration of c. 16 (±2) µmol $kg^{-1}$ through additions of calculated amounts of HCl (3.571 molar). In the constant-pH experiments, pH was adjusted to 7.74 (± 0.004) or 8.34 (± 0.008) by adding 2 mmol $kg^{-1}$ of 2-[-4-(2-hydroxyethyl)-1-piperazinyl]-ethanesulfonic acid (HEPES, adjusted to target $pH_f$ levels).

Carbonate chemistry in the constant-$CO_2$ experiment was determined by measuring TA and $pH_f$, while in both constant-pH experiments it was determined from $pH_f$ and DIC. Carbonate chemistry samples were taken at the beginning and the end of the experiments. Samples for TA were filtered (0.7 µm), poisoned with saturated HJgCl2 solution (0.5 ‰ final concentration) and stored at 4°C until measured (Dickson et al., 2003). TA values higher

than 4700 µmol $kg^{-1}$were outside the range that can be accurately determined with the applied method and therefore diluted with double deionized water as described in Bachet al.(2012).

Samples for DIC were sterile-filtered (0.2 µm) by gentle pressure into 4 ml borosilicate bottles, made air-tight without headspace and subsequently measured as described in Stoll et al. (2001). DIC samples lower than 1000 or higher than 3000 µmol $kg^{-1}$ could not be reliably measured with the applied method and were therefore either diluted or concentrated (see Bach et al., 2011, 2012).

Samples for $pH_f$ were measured potentiometrically at 15°C with separate glass and reference electrodes (METROHM) calibrated with reference seawater, certified for TA and DIC (supplied by Prof. A.Dickson, La Jolla, CA, USA; see Bach et al., 2011, 2012 for details).

Carbonate chemistry parameters that were not directly measured were calculated from two measured values (DIC and TA or DIC and $pH_f$) and known salinity, temperature, and phosphate concentrations with the software CO2SYS (Lewis & Wallace, 1998) using equilibrium constants determined by Roy et al. (1993). Biological response data are plotted against the means of the initial and final values of the carbonate chemistry. Error bars in plotted carbonate chemistry parameters denote the mean change of the three replicates of the particular carbonate chemistry parameter from the beginning of the experiment to the end.

## Sampling, measurements and calculations of growth, organic, and inorganic carbon production rates

Sampling started 2 h after the onset of the light period and lasted not longer than 2.5 h. Duplicate samples for total particulate carbon (TPC) and particulate organic carbon (POC) were filtered (200 mbar) on to precombusted (5 h at 500°C) GF/F filters. To remove HEPES from the filters of the constant-pH experiments, samples were rinsed with 60 ml of artificial seawater medium supersaturated with respect to calcium carbonate and free of HEPES buffer immediately after filtration. Filters were stored at -20°C until measurements were carried out. POC filters were placed for 2 h in a desiccator containing fuming HCl to remove all calcite and then dried for c. 6h at 60°C. TPC filters were dried under the same conditions but without the acid treatment. TPC and POC analyses were performed using an elemental analyser (HEKATECH, Wegberg, Germany) combined with an isotope ratio mass spectrometer (FINNIGAN, Schwerte, Germany). Particulate inorganic carbon (PIC) was calculated as the difference between TPC and POC.

Cell numbers were determined with a Coulter Counter (Beckman Coulter, Krefeld, Germany) at the beginning and the end of the experiments c. 4 h after the onset of the light period. Growth rates (l) were calculated as

$$\mu = \frac{\log_e(t_{fin}) - \log_e(t_0)}{d} \qquad \text{Eqn 2}$$

where $t_0$ and $t_{fin}$ are the cell numbers at the beginning and the end of the experiments, respectively, and d is the growth period in days. POC and PIC production rates were calculated by multiplying growth rates with the cellular POC or PIC contents.

Treatments were further analyzed by scanning electron microscopy (SEM) and cross-polarized light microscopy to confirm the presence or absence of internal coccoliths (Bach et al., 2012). Cells were considered to be actively calcifying if coccoliths were present.

For gene expression analysis, c. 10 million cells were filtered (200 mbar) onto polycarbonate filters with a pore size of 0.8 µm and subsequently rinsed off the filters with 1 ml RNAlater (Qiagen). This cell suspension was kept on ice until storage at -20°C.

## Quantitative reverse-transcriptase polymerase chain reaction (qRT-PCR)

Quantitative reverse-transcriptase polymerase chain reaction was performed for 15 target genes (Table 1). Each sample was measured in triplicate. Experimental procedures were performed as described previously (Mackinder et al., 2011). Primers were designed using expressed sequence tag (EST) clusters from von Dassow et al. (2009), the *E. huxleyi* Genome Project (http://genome.jgi-psf.org/Emihu1/Emihu1.home.html) or from the current literature (Supporting Information, Table S1). Efficiency curves for each primer pair were generated using serial dilutions on pooled cDNA from all samples. All primers except beta-carbonic anhydrase (bCA) had efficiencies between 90 and 105% and generated curves with $R^2$ values > 0.99. ßCA efficiency remained undetermined as a result of the low cycle threshold (CT) values of pooled cDNA even at undiluted levels. For relative expression calculations, its efficiency was assumed to be 100%. This assumption results in a potential decrease in the accuracy of the absolute fold changes, but the trend of expression and the order of magnitude will remain unaffected. For each sample, 2–20 ng of RT RNA were analyzed in technical triplicates. For each primer pair, all samples were analyzed across three plates, and in order to allow for the correction of between-plate variation two standards in triplicate were run on each plate. GeNorm (Vandesompele et al., 2002) was used to test the stability of four potential endogenous reference genes (ERGs).

Analysis of qRT-PCR data was done using an efficiency corrected $\Delta\Delta C_t$ method, normalizing to the geometric mean of three ERGs (Vandesompele et al., 2002). For each gene, all samples were plotted relative to the sample with lowest expression from all three experiments. The sample with the lowest expression level was normalized to 1, allowing the expression ratios between samples to be easily identified.

## Statistical analysis

We tested if the carbonate chemistry had a statistically significant effect ($P < 0.05$) on individual physiological and molecular response parameters with either a one-factorial analysis of variance (ANOVA) using Statistica (Statsoft, Hamburg, Germany) in case the data subsets were normally distributed, or with a permutational multivariate analysis of variance (PERMANOVA) using Primer 6 in case they were not. Normality was tested with Shapiro–Wilk's test ($P = 0.05$). Nonnormally distributed subsets were Box–Cox-transformed. Subsets that remained nonnormally distributed were analyzed with the PERMANOVA.

ANOVA: The difference of individual treatments within an experiment was tested with Tukey's HSD *post-hoc* test (P values from *post-hoc* tests are denoted by $P_{post\ hoc}$).

Homogeneity of variance was tested using Levene's test and was accepted if the P-value was > 0.05. Where P was smaller, the significance level (P-value of the ANOVA and the *post-hoc* test) was decreased to 0.01. Subsets treated this way are marked in Table S2.

PERMANOVA: A resemblance matrix was created using the Euclidian distance function and further processed with a one-factorial PERMANOVA design choosing type III partitioning of the sum of squares. In cases where statistically significant differences were detected, a pairwise comparison of treatments (analog to a *post-hoc* test) was conducted in a second PERMANOVA run. The numbers of permutations for each run are given in Table S2. In pairwise PERMANOVA runs, these numbers were not sufficiently high (< 100) to get reasonable results for P, so that an additional Monte Carlo test was conducted. Significance levels of the PERMANOVA analysis are the same as for the ANOVA, but by convention are termed P(perm) for the permutation P-value and $P_{post\ hoc}$(MC) for the Monte Carlo P-value to distinguish them.

**Results**

Growth and POC production rates are sensitive to low $CO_2$ (and $HCO_3^-$) and to low pH, but not to elevated $CO_2$ To determine the importance of individual components of the carbonate system for *E. huxleyi* physiology, cells were grown in three separate experiments at constant $pH_f$ (7.74 and 8.34) and constant $CO_2$ (16 µmol $kg^{-1}$). Fig. 1 shows how the carbonate system changed within the three experiments. By maintaining relatively low cell concentrations, changes in carbonate chemistry as a result of biological processes were kept to a minimum over the time of the experiments. This is indicated by the error bars in Fig. 1 with the corresponding values in Table S3.

Within the ranges examined, growth and POC production rates were primarily influenced by changes in carbonate chemistry from low to intermediate $HCO_3^-$ (160–2000 µmol $kg^{-1}$) and $CO_2$ (0.8–20 µmol $kg^{-1}$) (Fig. 2) with neither pH nor $CO_2^-{}_3$ having a pronounced influence (Fig. S1). Growth rates increased in all experiments with increasing concentrations of $HCO_3^-$ and $CO_2$ until reaching maximum rates of c. 1.1 $d^{-1}$ where further $CO_2$ or $HCO_3^-$ increases had no effect on growth rates. The constant-pH experiments allow us to differentiate between the effects of $CO_2$ and $HCO_3^-$ on growth rate. $CO_2$ demonstrates a good correlation with growth rate in both constant-pH experiments, whereas the influence of $HCO_3^-$ on growth rate is more variable (Fig. 2a,b), suggesting that $CO_2$ is the principal factor responsible for growth inhibition below a [$CO_2$] of c. 7.5 µmol $kg^{-1}$ (Fig. 2b). No effect of pH on growth rate was observed in the constant-pH treatments (7.74 and 8.34). However, at constant $CO_2$, growth rates are significantly lower at pH 7.58 than at pH 7.83 ($P_{post\text{-}hoc}$ = 0.009), which cannot be explained by a decrease in [$CO_2$] or [$HCO_3^-$] (Fig. 2a,b). Thus, below $pH_f$ 7.74, [$H^+$] appears to have a direct negative influence on growth rate.

Particulate organic carbon production rates in both constant-pH experiments were highly sensitive to $HCO_3^-$ and $CO_2$ when the concentrations dropped below c. 2000 and 10 µmol $kg^{-1}$, respectively (Fig. 2c,d). The rates appear to correlate best to $CO_2$ at concentrations < c. 5 µmol $kg^{-1}$, although there are limited data points in this range. At a constant $CO_2$, the lowest $HCO_3^-$ treatment also showed significantly lower POC production rates than at intermediate $HCO_3^-$ ($P_{post\ hoc}$ = 0.002, Fig. 2c). At $HCO_3^-$ concentrations > c. 2000 µmol $kg^{-1}$ POC production rates display a slight but significant decrease of c. 20% at a constant $pH_f$ of 8.34 and 10% at a constant $pH_f$ of 7.74 up to the highest $HCO_3^-$ concentrations (Fig. 2c; pH

8.34, $P_{post\ hoc}$ <0.001; pH 7.74, $P_{post\ hoc}$ (MC) = 0.004). In summary, POC production showed no clear overall correlation with any of the carbonate chemistry parameters, but appears to be driven by $CO_2$ in the very low $CO_2$ range (< c. 5µmol $kg^{-1}$) and decreased by $HCO_3^-$ at concentrations > 2000 µmol $kg^{-1}$.

At low DIC, C:N ratios decreased significantly in the constant-pH experiments, which appear to be driven primarily by a reduction in $CO_2$ (Table S2). This is supported by no significant changes at constant $CO_2$ (Table S2). Differences in C:N between treatments probably reflect variable cellular amounts of nitrogen-free relative to nitrogen-rich organic compounds. As 40–60% of the total cellular carbon in *E. huxleyi* is in the form of lipids (Fernandez et al., 1994), the decrease in C:N is likely to reflect reduced assimilation of lipids and polysaccharides at low DIC.

## Calcification is primarily driven by $HCO_3^-$ and does not act as a CCM

Calcification rates (PIC production) increased similarly in all experiments with increasing [$HCO_3^-$] (Fig. 2g). Maximum calcification rates at constant $pH_f$ values of 8.34 and 7.74 were identical, but were reached at lower $CO_2$ and higher $CO_2^-{}_3$ at a constant $pH_f$ of 8.34, indicating that calcification is not primarily dependent on [$CO_2$] or [$CO_2^-{}_3$] (Figs 2h, S1h). A limited control of calcification by [$CO_2$] is further supported by the decrease in calcification rates found in the constant-$CO_2$ experiment. Here, calcification rates would have to remain constant if [$CO_2$] were of primary importance. No signs of calcification could be found in the two lowest $HCO_3^-$ treatments at a constant $pH_f$ of 7.74 and in two replicates of the lowest $HCO_3^-$ treatment at constant $CO_2$ (Table 2). In these treatments, calcite saturation ($\Omega_{calcite}$) is < 0.31, so post-production dissolution could potentially have taken place. However, cross-polarized light microscopy and scanning electron microscopy show the absence of internal coccoliths under these conditions, indicating that the production of coccoliths is inhibited (Bach et al., 2012).

Low DIC therefore results in a decrease in growth rate and POC production as well as in calcification (Figs 2, S2). However, PIC production appears to be the most sensitive to low DIC, with low calcification rates observed in several low-DIC conditions where there was no appreciable effect on POC production and growth rate (Fig. S2). This indicates that POC production is prioritized over PIC production under Ci limitation (Fig. S2), and suggests that reducing calcification rate may enable cellular resources (such as those relating to $HCO_3^-$ uptake) to be used for photosynthesis. Calcification is clearly not operating as a CCM at low DIC, as in this case we would expect a stimulation of calcification at low DIC.

## At a genetic level, the CCM is up-regulated only at low $CO_2$ and is not induced at current ocean $CO_2$ concentrations

In order to identify the molecular basis of the physiological response of *E. huxleyi* to the individual carbonate system parameters, 15 genes with putative roles in carbon transport, pH homeostasis and biomineralization were chosen for investigation (Table S1). The measurement of relative transcript abundance was chosen as the most suitable approach to allow the expression profiles of multiple genes to be accurately determined. Although transcript abundance is not a direct measurement of protein abundance or activity, it gives a good insight into the cellular demand for specific proteins and provides a strong foundation for the further characterization of genes related to a particular cellular process. All genes are

normalized to three endogenous reference genes (ERGs; ACTIN, α-TUBULIN and EFG1-α) with expression plotted relative to the lowest expression level, which is set to one.

Plotting gene expression against DIC indicates the transcriptional response to changes in total DIC (Fig. 3, Table S3). Out of the 15 genes investigated, 11 showed a marked increase in expression when the cells became DIC-limited (DIC < 1000 μmol $kg^{-1}$) but showed no repression above this concentration. This corresponds to [$CO_2$] and [$HCO_3^-$] thresholds of c.7.5 and 800 μmol $kg^{-1}$, respectively, below which CCM gene up-regulation occurs (Fig. 4a, b). Both of these values are approximately half that of average current oceanic values (i.e. similar to pre-industrial values), suggesting that the *E. huxleyi* CCM, at least in this strain, is actually only induced at DIC concentrations lower than ambient.

Of the selected genes with putative roles in DIC transport, AEL1 (anion exchanger like 1, belonging to the solute carrier 4 (SLC4) family), αCA1 (alpha-carbonic anhydrase 1), δCA (deltacarbonic anhydrase 1) and *rubisco* (RubisCO large subunit) showed a significant DIC limited up-regulation between four and 11-fold (Table 1, Fig. 3a). Two genes, ßCA and LCIX (low $CO_2$ induced gene X), had a large response at low DIC, with a respective 450- and 180-fold up-regulation at the lowest DIC value in the constant-$pH_f$ (= 8.34) experiment relative to the treatment with the lowest expression (Table 1, Fig. 3e,f). ßCA encodes a putative carbonic anhydrase responsible for catalysing the interconversion of $CO_2$ and $HCO_3^-$, whereas LCIX exhibits similarity to the *Chlamydomonas* LCIB protein, which is located in the chloroplast and plays a crucial role in $HCO_3^-$ uptake (Miura et al., 2004; Wang & Spalding, 2006). Furthermore, ßCA showed a highly correlated expression with LCIX ($R^2$ > 0.99, data not shown), indicating that these genes could be under the same transcriptional control.

Of the putative $H^+$ transport-related genes, CAX3 ($Ca^{2+}/H^+$ exchanger 3), NhaA2 ($Na^+/H^+$ exchanger 2), ATPVc′/c (vaculoartype $H^+$ pump) and PATP (plasma membrane-type $H^+$ pump) showed a 4–7.5 fold up-regulation (Table 1, Fig. 3b). Four genes with potential roles in $H^+$ and DIC transport, HVCN1 ($H^+$ channel), AQP2 (aquaporin 2), αCA2 (alpha-carbonic anhydrase 2), and γCA (gamma-carbonic anhydrase), showed no significant transcriptional response over the carbonate system range tested (Fig. 3c; Table S2). Above 1000 μmol $kg^{-1}$, DIC changes in gene expression of most investigated genes was minimal with no repression of DIC-responsive genes, but a small but significant decrease ($P_{post\ hoc}$ = 0.02) seen in GPA expression > c.2000 μmol $kg^{-1}$ (Fig. 3d).

## The CCM is responsive to $CO_2$ and $HCO_3^-$ but not to pH

An understanding of the regulation of the *E. huxleyi* CCM may provide important information about its mode of operation and cellular function. An examination of the individual carbonate system parameters indicated that the expression of these genes correlates closely with [$CO_2$] and [$HCO_3^-$] at low DIC (Fig. 4a,b). This indicates that although pH and $CO_2^-{}_3$ may have a synergistic effect with other factors on the expression of some genes, they do not appear to be the main parameters of the carbonate system driving the genetic responses (Fig. 4c,d). Table 1 summarizes the responses of the investigated genes along with their putative or confirmed function and potential cellular locations.

## Transcriptional response to reduced calcification

Previously we demonstrated that the expression of several genes with putative roles in DIC, $Ca^{2+}$ and $H^+$ transport (AEL1, CAX3 and ATPVc′/c) show a close correlation with calcification

rate, suggesting that these genes play a direct role in the calcification process (Mackinder et al., 2011). When calcification was inhibited by the removal of $Ca^{2+}$, the expression of these calcification-associated genes was strongly repressed (Mackinder et al., 2011). However, in the present study, these genes were all induced at low DIC (Fig. 3), whereas calcification was inhibited. This indicates that these genes may play a dual role within the cell, supporting calcification under ambient conditions but switching to support photosynthesis when DIC becomes limiting.

## Discussion

### Growth and calcification responses to the carbonate system

The predicted changes in the ocean's carbonate system caused by increasing atmospheric $CO_2$ may have multiple impacts on coccolithophore physiology (Riebesell & Tortell, 2011). Using experimental manipulation of the carbonate system, we show that individual aspects of *E. huxleyi* physiology can be attributed to separate components of the carbonate system.

Growth rates presented in this study correlate closely to [$CO_2$] (Fig. 2a), with $pH_f$ having a significant negative impact below values of c. 7.7 (Fig. S1a). Although POC production does not show such a clear coupling to [$CO_2$] as growth rates (Fig. 2d), it also responds negatively to $pH_f$ when it drops below c. 7.7. A similar regulation of pH and $CO_2$ on growth and POC production was also seen in Bach et al. (2011) with a linear decrease from a $pH_f$ of c. 7.7–7.0 and $CO_2$ dependence above a $pH_f$ of 7.7. However, a study by Buitenhuis et al. (1999) saw no clear tightly coupled correlation between *E. huxleyi* growth rate and [$CO_2$]. Instead, the authors suggested that both $CO_2$ and $HCO_3^-$ are important for growth rates. The reason behind this discrepancy is unclear, although it should be kept in mind that threshold values for individual carbonate system components may differ between strains and may be modulated by light conditions (Langer et al., 2009; Rokitta & Rost, 2012).

Calcification rates are tightly coupled to [$HCO_3^-$] (Fig. 2g), suggesting that $HCO_3^-$ is the primary carbon source used for $CaCO_3$ precipitation in *E. huxleyi*. This is in agreement with previous studies (reviewed in Paasche, 2001). Simulated ocean acidification has been shown to affect coccolithophore calcification mostly negatively (Riebesell & Tortell, 2011). By comparing ocean acidification with constant-pH experiments, Bach et al. (2011) showed that it is the increase in $H^+$ at elevated $CO_2$ that negatively affects calcification rates of *E. huxleyi*. It is also known that intracellular pH in coccolithophores is particularly sensitive to changes in external pH (Suffrian et al., 2011; Taylor et al., 2011). Under these considerations, it could be expected that calcification rates would remain consistently lower throughout the constant $pH_f$ = 7.74 experiment compared with the constant $pH_f$ = 8.34 experiment. Surprisingly, however, this is not the case. Instead, maximum calcification rates are similar in both constant-pH experiments (Fig. 2g,h). This indicates that the direct negative effect of high [$H^+$] on calcification rates may at some point be overcome by increasing availability of $HCO_3^-$ substrate. This is further supported by our finding that higher [$HCO_3^-$] was necessary to initiate calcification when [$H^+$] in the seawater medium was higher (Table 2). Considering carbonate chemistry conditions of the past, this might provide a further explanation as to why coccolithophores were able to thrive in the early Mesozoic era, a time that was characterized by relatively low sea water pH (as low as pH 7.7) and high DIC substrate (up to 5000 µmol $kg^{-1}$; Ridgwell, 2005).

## The nature and regulation of the CCM

Previous mass spectrometrically based work by Rost et al. (2003) showed that *E. huxleyi* operates a regulated CCM but gave no indication of the mechanism. Our results support the presence of a regulated CCM and furthermore have identified several of its molecular components, the carbonate species to which it responds, the threshold at which it is induced, and its possible interactions with calcification.

The transcriptional data identify the genetic basis of a CCM in *E. huxleyi* with a clear up-regulation in multiple putative CCM-related genes as DIC becomes limiting for growth, POC and PIC production (Fig. 3, Table 1). The majority of genes were up-regulated when $HCO_3^-$ or $CO_2$ dropped below c. 800 and 7.5 µmol $kg^{-1}$, respectively. Interestingly, most of the DIC-responsive genes were not further repressed at $CO_2$ > c. 7.5 µmol $kg^{-1}$ ([$HCO_3^-$] c. 800 µmol $kg^{-1}$); this indicates a potential basal level of the CCM, with a low amount of active DIC transport taking place even when growth rates and POC production are saturated. The presence of active transport at ambient $CO_2$ and $HCO_3^-$ is supported by Schulz et al. (2007), who showed active DIC uptake even at ambient conditions.

Photosynthetic $O_2$ evolution curves and $^{14}C$ incorporation studies have indicated that photosynthesis is not saturated at ambient $CO_2$ (Paasche, 1964; Herfort et al., 2002; Rost et al., 2003). This is not supported by our data with growth rates and organic carbon fixation both saturated at or below ambient [$CO_2$]. However, these differences could theoretically be attributed to the different light intensities used between the studies and to the fact that $O_2$ evolution is a measurement of photosystem II activity, not a direct measurement of $CO_2$ fixation. Furthermore, these thresholds may vary between strains, as seen with strain-specific responses in calcification and growth to changing carbonate chemistry (Langer et al., 2009). These responses do not necessarily indicate that the underlying cellular mechanisms differ between strains, but most likely highlight differences in the regulation of cellular processes, such as calcification. This is further supported by an optimum curve response, with different strains and species having varying optimum calcification rates in relation to $pCO_2$, but the overall response (i.e. the shape of the curve) being very similar (Langer et al., 2006, 2009; Ridgwell et al., 2009; Bach et al., 2011; Krug et al., 2011). However, a greater understanding at the molecular level of the response of different *E. huxleyi* strains and coccolithophore species to changes in carbonate chemistry is critical to extrapolate our data to other coccolithophores.

The CCM of *E. huxleyi* shows a number of differences from those of other partially characterized eukaryotic algae. One outstanding feature is its low affinity for $CO_2$ (Rost et al., 2003) with a $K_{1/2}$ for $CO_2$ that is several-fold higher than the $K_{1/2}$ for the prymnesiophyte *Phaeocystis globosa* and several diatom species (Johnston & Raven, 1996; Rost et al., 2003; Trimborn et al., 2009). Another feature of the *E. huxleyi* CCM is that up-regulation of molecular components seems to occur only when very low $CO_2$ concentrations are reached. This is strikingly different from diatoms and *Chlamydomonas*, where molecular CCM components are already strongly induced at ambient $CO_2$ and even above (Harada et al., 2005; Brueggeman et al., 2012).

Although the *E. huxleyi* CCM may be of a lower affinity, the basic components appear to be similar to other eukaryotic algae. CAs play fundamental roles within algal CCMs, and CAs associated with the CCM are generally up-regulated under carbon limitation (Badger, 2003;

Raven & Giordano, 2009). Genome analysis shows that *E. huxleyi* has nine putative CAs belonging to the a, b, c and d families. This CA composition demonstrates strong similarities with *Chlamydomonas*, which has 10 putative CAs in its genome belonging to the a, b and c families (Spalding, 2008). It is also very similar to the diatom CA repertoire, with *Phaeodactylum tricornutum* also having nine CAs distributed across the same four families (Tachibana et al., 2011). Diatoms also possess multiple homologs to AEL1. The characterization of *P. tricornutum* SLC4-2 shows that it is induced at low $CO_2$, localizes to the plasma membrane and stimulates $HCO_3^-$ uptake and photosynthesis (Nakajima et al., 2013). Wolf PSORT predicts a plasma membrane location for AEL1 (Table 1) and its low $HCO_3^-/CO_2$-dependent expression suggests a related function in *E. huxleyi*.

Localized intracellular pH gradients and regulation are thought to be a fundamental part of CCMs (Raven, 1997). The increased expression of putative proton pumps (ATPVc′/c and PATP) and cation/$H^+$ exchangers (NhaA2 and CAX3) suggests an increased demand of these transporters to maintain pH homeostasis, membrane potential or alter compartmental pH in order to promote changes in $CO_2$ : $HCO_3^-$ ratios. More alkaline regions would maintain DIC as $HCO_3^-$, which is one million times less permeable to membranes than $CO_2$ (Moroney et al., 2011). This could prevent $CO_2$ loss via diffusion across membranes, while more acidic regions in the proximity of RubisCO would result in a shift to $CO_2$ (Raven, 1997).

Although $HCO_3^-$ use appears to become increasingly important at low DIC (Rost et al., 2003; Schulz et al., 2007; AEL1 up-regulation at low DIC shown here), growth rates are ultimately determined by $CO_2$ (Fig. 2b). By operating a CCM, the cell actively accumulates $HCO_3^-$ and $CO_2$ at a higher concentration in the proximity of RubisCO than externally. DIC has to be presented to RubisCO as $CO_2$, so ultimately $HCO_3^-$ accumulated for carbon fixation will have to be converted to $CO_2$. If the external $CO_2$ concentration is very low, the diffusion gradient from the chloroplast to the outside will be large and leakage increases (Rost et al., 2006). Leakage in *E. huxleyi* has been measured to be c. 79% at ambient $CO_2$ (Schulz et al., 2007) and shown to increase as $CO_2$ decreased (Rost et al., 2006). Thus, external [$CO_2$] largely determines how much accumulated DIC stays within the cell as a result of the strong inside-to-out $CO_2$ gradient and high permeability of membranes to $CO_2$.

## Calcification as a CCM

Coccolithophores have maintained calcification since coccoliths appeared in the fossil record c. 220 million yr ago (Bown et al., 2004). A proposed role for the maintenance of calcification in coccolithophores is to support photosynthesis by using $H^+$ generated by the production of calcium carbonate from bicarbonate (Paasche, 2001). Whilst carbon fixation by photosynthesis and calcification can occur at a similar rate within a cell, there is increasing evidence suggesting that the two processes are not tightly linked. It is possible to inhibit calcification by limiting calcium (Herfort et al., 2004; Trimborn et al., 2007; Leonardos et al., 2009) or DIC (Buitenhuis et al., 1999; this study), whilst photosynthesis, growth and POC production rates remain unaffected (Trimborn et al., 2007; constant-$CO_2$ experiment of this study). Photosynthesis therefore appears to have no mechanistic dependence on calcification (Leonardos et al., 2009). Our data support this and strongly suggest that calcification does not function as a CCM at low DIC.

Moreover, our data reveal that calcification is actually inhibited at low DIC, rather than induced. Current evidence indicates that coccolithophores largely use $CO_2$ for

photosynthesis and $HCO_3^-$ for calcification (reviewed in Paasche, 2001), which is supported by our own observations. Thus, inhibition of calcification would enable the cell to utilize the $HCO_3^-$ normally acquired for calcification as a substrate for photosynthesis. Here we provide the first transcriptional dataset in support of this hypothesis. We found that the expression of three putative calcification-related ion transporters was elevated under limiting DIC, whilst calcification was inhibited. For example, assuming AEL1 functions as a plasma membrane $HCO_3^-$ transporter in *E. huxleyi*, as with SLC4-2 in diatoms, under normal conditions it most probably acts to transport $HCO_3^-$ into an intracellular pool for calcification (Fig. 5a). This is supported by AEL1 expression being repressed when calcification is inhibited by calcium limitation or in noncalcifying strains (Mackinder et al., 2011). However, under low $CO_2$ and $HCO_3^-$ availability, AEL1 is induced, whereas calcification is inhibited. This suggests that there is an increased need for $HCO_3^-$ transport at low DIC, but that this $HCO_3^-$ is diverted away from the coccolith vesicle into the chloroplast for photosynthetic carbon fixation (Fig. 5b). Further functional characterization and localization of AEL1 and other CCM/calcification components is critical to validate this model and to fully understand this process at the molecular level.

## Extrapolation to the real ocean

The expression data indicate an up-regulation of the CCM occurring at low DIC ([$CO_2$] c. 7.5 µmol $kg^{-1}$), suggesting that an inducible CCM is redundant in this *E. huxleyi* strain under current oceanic [$CO_2$] (c. 16 µmol $kg^{-1}$). However, in their natural habitat, it is possible that cells sporadically experience [$CO_2$] < 7.5 µmol $kg^{-1}$, in particular at the end of a bloom where [$CO_2$] is reduced as a result of photosynthetic carbon drawdown. Values as low as c. 5 µmol $kg^{-1}$ were seen in a mesocosm experiment where an *E. huxleyi* bloom occurred after a *Phaeocystis* sp. and diatom bloom (Purdie & Finch, 1994). Furthermore, [$CO_2$] was significantly lower before the onset of anthropogenic $CO_2$ release c. 200 yr ago, so that limiting DIC concentrations might have occurred more frequently in the past. A third aspect, which has to be considered, is a possible variability in the threshold DIC concentration below which the CCM is up-regulated. Variable thresholds either could result from strain-specific differences between *E. huxleyi* clones (Langer et al., 2009) and/or could be altered by culture conditions (Rokitta & Rost, 2012). At very high light conditions, for example, it is possible that the CCM becomes up-regulated at a higher $CO_2$ threshold, owing to the cell having a larger DIC demand. Finally, the necessity of an inducible CCM in *E. huxleyi* can only be reliably determined by in field experiments where regulation patterns are investigated in *in situ* conditions.

Increased $pCO_2$ has been shown to affect intracellular processes like calcification and photosynthesis in coccolithophores (Riebesell et al., 2000; Langer et al., 2006, 2009). In contrast to these physiological responses, our data suggest that the regulatory response to these changes at a genetic level is very limited. $CO_2$ and $HCO_3^-$ only enhanced transcription of genes at concentrations significantly below those currently experienced and well below concentrations predicted in the near future. Furthermore, none of the investigated genes – even putative $H^+$ pumps – were responsive to increasing sea water [$H^+$]. There are two possible explanations for this lack of regulatory response: we have simply missed the critical pH and high $CO_2$ responsive genes; or *E. huxleyi* does indeed entirely lack a regulatory machinery to cope with ocean acidification. The former can only be addressed in similar future studies that investigate the whole transcriptome. However, if future studies support the

latter then the inability to regulate to changing pH could offer an explanation as to why calcification and photosynthesis are negatively affected below certain pH thresholds.

The novel approach applied in this study has allowed us to tease out the complexities of, and interactions between, photosynthesis and calcification in the ecologically important phytoplankton, *E. huxleyi*, and their responses to changing $pCO_2$. The data presented provide a significant step forward in understanding the underlying cellular and molecular mechanisms of these processes, providing strong evidence that calcification does not function as a CCM and indicating that *E. huxleyi* may have evolved mechanisms to deal with limiting rather than elevated $pCO_2$.

**Acknowledgements**

Silke Lischka is acknowledged for support on statistics and Janett Voigt for support during sampling. Furthermore, we thank three anonymous reviewers for their valuable comments, which helped to improve the manuscript. The work was funded by CalMarO a FP7 Marie Curie Initial training network and the Federal Ministry of Education and Research (Bundesministerium für Bildung und Forschung; 03F0608A) in the framework of the Biological Impacts of Ocean Acidification (BIOACID) project (subproject 3.1.1).

**Figures and tables**

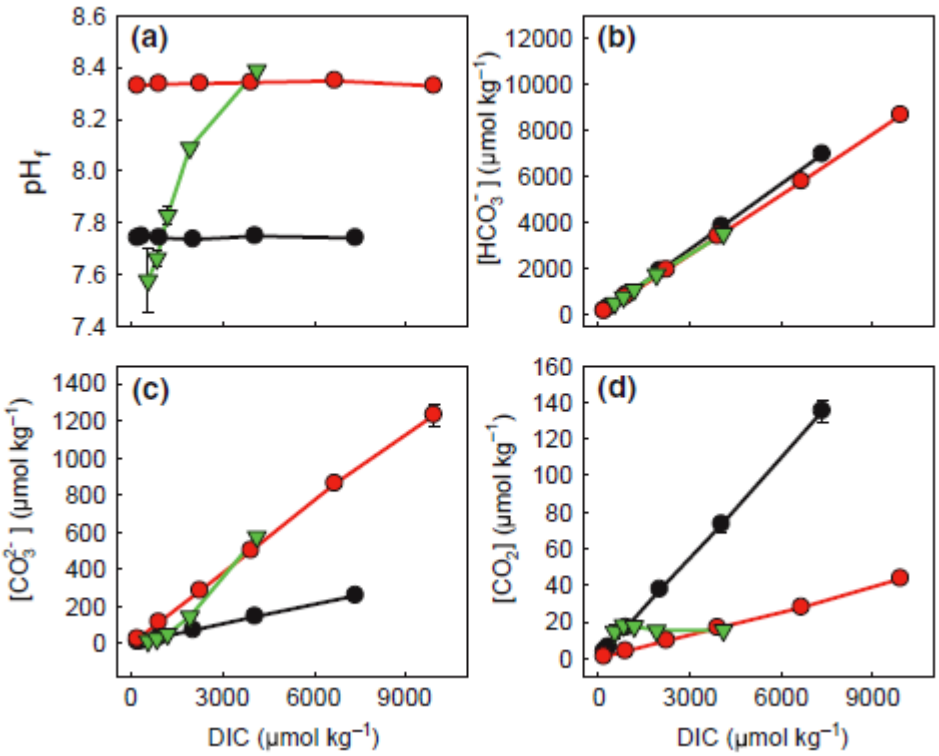


**Fig. 1** Physiologically relevant carbonate chemistry parameters in relation to dissolved inorganic carbon (DIC). (a) $pH_f$. (b) [$HCO_3^-$]. (c) [CO-3 ]. (d) [$CO_2$]. Error bars account for the mean change (mean of triplicates) of the particular carbonate chemistry parameter over the course of the experiments. Black circles, constant $pH_f$ = 7.74; red circles, constant $pH_f$ =

8.34; triangles, constant CO2. Note that error bars are in most cases masked by symbol size.

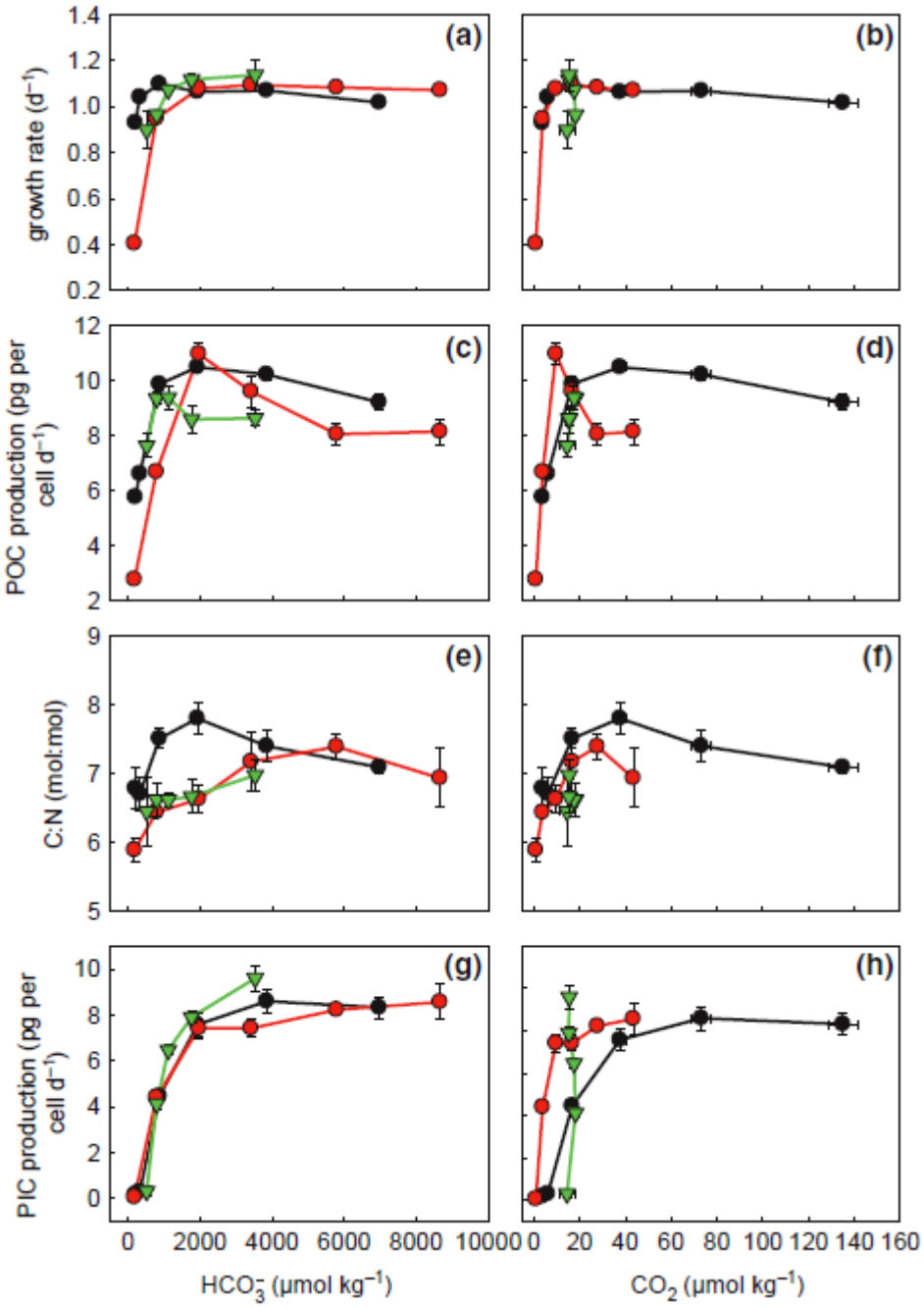


**Fig. 2** Physiological response parameters for *Emiliania huxleyi* in relation to [$HCO_3^-$] (left column) and [$CO_2$] (right column). (a, b) Growth rates; (c, d) particulate organic carbon (POC) production; (e, f) C : N ratio; (g, h) particulate inorganic carbon (PIC) production. Black circles, constant $pH_f$ = 7.74; red circles, constant $pH_f$ = 8.34; triangles, constant $CO_2$. Vertical error bars denote the standard deviation of three replicates. Horizontal error bars show the mean change in [$HCO_3^-$] or [$CO_2$] (mean of triplicates) from the beginning to the end of the experiments.

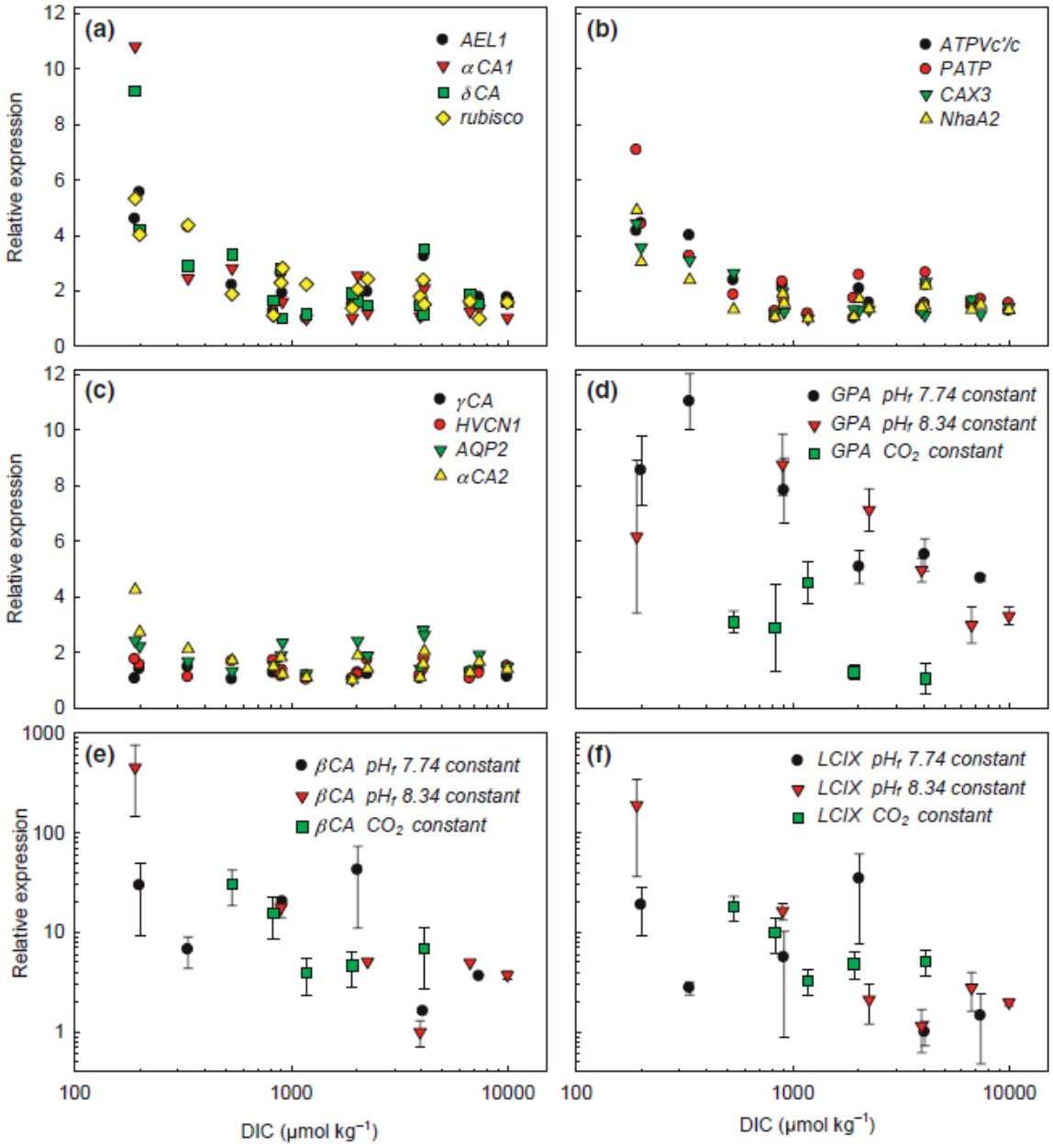


**Fig. 3** Relative expression of investigated *Emiliania huxleyi* genes plotted against dissolved inorganic carbon (DIC). (a, b) Inorganic carbon transport and H+ transport genes that were significantly up-regulated ($P < 0.05$) at DIC < c. 200 µmol $kg^{-1}$ relative to DIC > 1000 µmol $kg^{-1}$. Panel (c) shows nonresponsive genes ($P > 0.05$) over the DIC ranges tested. Panels (a)–(c) are combined data from the constant $pH_f$ 7.74, constant $pH_f$ 8.34 and constant $CO_2$ experiments for each gene. Error bars have been omitted to improve clarity but standard deviations are listed in Table S3. Plots in (d)–(f) show expression of GPA, ßCA, and LCIX in the three individual experiments with standard errors shown. Note the logarithmic y-axis for plots in (e) and (f). The absence of error bars for some samples in (e) is the result of undetectable abundances of ßCA transcripts in some of the biological replicates. (d) shows GPA, which was significantly downregulated at high (> 2000 µmol $kg^{-1}$) DIC compared with low (< 400 µmol $kg^{-1}$) DIC. Note that fold changes and corresponding significances are shown in Tables 1 and S2. AEL1, anion exchanger like 1; αCA1, alphacarbonic anhydrase 1; δCA, delta-carbonic anhydrase 1; *rubisco*, RubisCO large subunit; CAX3, $Ca^{2+}/H^{+}$ exchanger

3; NhaA2, $Na^+$/ $H^+$ exchanger 2; ATPVc′/c, vaculoar-type $H^+$ pump; PATP, plasma membrane-type $H^+$ pump; HVCN1, $H^+$ channel; AQP2, aquaporin 2; αCA2, alpha-carbonic anhydrase 2; γCA, gamma-carbonic anhydrase; ßCA, beta-carbonic anhydrase; LCIX, low $CO_2$ induced gene X.

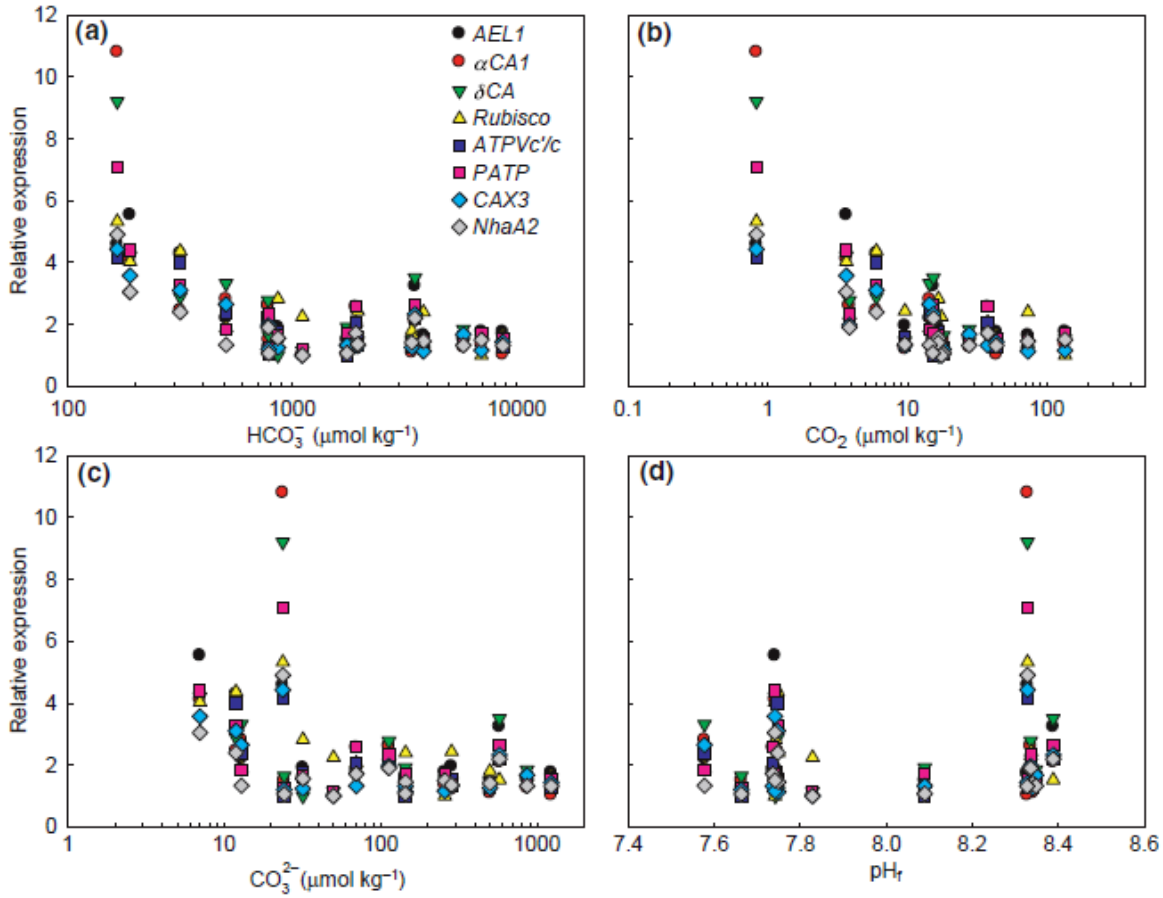


**Fig. 4** Plots of *Emiliania huxleyi* gene expression vs the individual components of the carbonate system for eight dissolved inorganic carbon (DIC)-responsive genes. Error bars have been omitted to improve clarity, but standard deviations are listed in Table S1: (a) vs. $HCO_3$; (b) vs $CO_2$; (c) vs $CO_3$; (d) vs $pH_f$. AEL1, anion exchanger like 1; αCA1, alpha-carbonic anhydrase 1; δCA, delta-carbonic anhydrase 1; *rubisco*, RubisCO large subunit; ATPVc′/c, vaculoar-type $H^+$ pump; PATP, plasma membrane-type $H^+$ pump; CAX3, $Ca^{2+}/H^+$ exchanger 3; NhaA2, $Na^+/H^+$ exchanger 2.

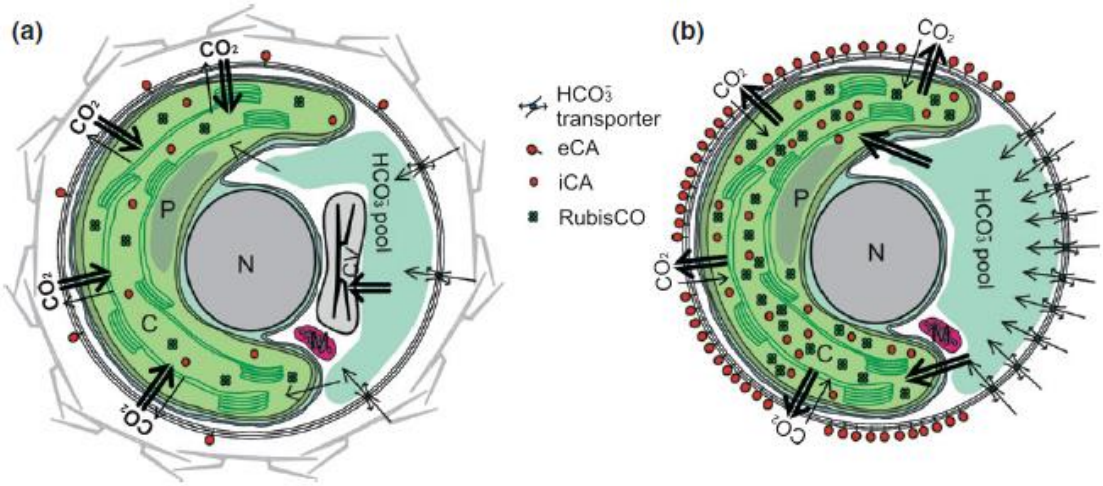


**Fig. 5** A conceptual model of inorganic carbon uptake in *Emiliania huxleyi* at high (a) and low (b) dissolved inorganic carbon (DIC). The model is based on the data presented in this manuscript and previous studies (see Table 3 for all assumptions within the model). (a) With increasing $CO_2$, the $CO_2$ gradient into the cell becomes, at some point, sufficient to saturate photosynthesis and maintain maximum particulate organic carbon (POC) fixation and growth rates. Hence $CO_2$ is the most important external substrate for photosynthesis at high $CO_2$, while $HCO_3^-$ is the main substrate for calcification with a putative $HCO_3^-$ exchanger AEL1 playing a key role. (b) At low $CO_2$, $HCO_3^-$ becomes more and more important as the inorganic carbon source for photosynthesis. Therefore, $HCO_3^-$ and its uptake mechanism shift from providing inorganic carbon for calcification to photosynthesis, leading to a reduction and, eventually, to a deactivation of calcification. Furthermore, the carbon-concentrating mechanism (CCM) (including the components shown: RubisCO, external and internal CAs) is up-regulated to support inorganic carbon supply. Although $HCO_3^-$ becomes the dominant external carbon source for photosynthesis, external $CO_2$ still strongly influences growth rates and POC fixation as a result of increasing $CO_2$ leakage as external $CO_2$ decreases (see text for details). C, chloroplast; P, pyrenoid; N, nucleus; M, mitochondrium; CV, coccolith vesicle; eCA, external carbonic anhydrase; iCA, internal carbonic anhydrase.

**Table 1** *Emiliania huxleyi* genetic response to carbonate system manipulations

| | | Correlation to carbonate system parameter | | | | Function and location | | |
|---|---|---|---|---|---|---|---|---|
| | | $CO_2$ (μmol $kg^{-1}$) | $HCO_3^-$ (μmol $kg^{-1}$) | $CO_3^{2-}$ (μmol $kg^{-1}$) | $pH_f$ | | | |
| Gene | Full name | <10 | <1000 | <50 | 7.5→8.5 | Putative function | Possible location – experimentally or by analogy | Predicted location by WoLF PSORT (Horton *et al.*, 2007) |
| *AEL1* | Anion exchanger like 1 | ↑5.5 | ↑5.5 | ↑5.5 | – | $HCO_3^-$ transport, probably coupled to $Na^+$, $Cl^-$ and/or $H^+$ transport | Plasma membrane or chloroplast. A diatom homolog has been shown to be plasma membrane-located (Nakajima *et al.*, 2013) | Plasma membrane |
| *αCA1* | α carbonic anhydrase 1 | ↑10.8 | ↑10.8 | ↑10.8 | – | $HCO_3^- + H^+ \leftrightarrow CO_2 + H_2O$ | αCAs are distributed throughout all kingdoms of life. In *Chlamydomonas* they are found in the periplasmic space and the thylakoid lumen (Spalding, 2008). In the diatoms *Phaeodactylum tricomutum* and *Thalassiosira pseudonana*, putative αCAs were located in the four layered plastid membrane system and inside the chloroplast, respectively (Tachibana *et al.*, 2011) | Nucleus, cytosol |
| *αCA2* | α carbonic anhydrase 2 | – | – | – | – | $HCO_3^- + H^+ \leftrightarrow CO_2 + H_2O$ | | Nucleus |
| *βCA* | β carbonic anhydrase | [a]↑454.7 | [a]↑454.7 | [a]↑454.7 | – | $HCO_3^- + H^+ \leftrightarrow CO_2 + H_2O$ | Plastid. Two βCAs have been localized to the stroma/pyrenoid in the diatom *P. tricomutum* (Tachibana *et al.*, 2011) | Chloroplast |
| *γCA* | γ carbonic anhydrase | – | – | – | – | $HCO_3^- + H^+ \leftrightarrow CO_2 + H_2O$ [b] (Soto *et al.*, 2006) | Mitochondrial location in Arabidopsis and *P. tricomutum*. γ-type CAs are found in the cyanobacteria carboxysome | Cytosol |
| *δCA* | δ carbonic anhydrase | ↑9.2 | ↑9.2 | ↑9.2 | – | $HCO_3^- + H^+ \leftrightarrow CO_2 + H_2O$ [b] (Soto *et al.*, 2006) | Plasma membrane location based on dinoflagellate δCAs (Lapointe *et al.*, 2008) | Plasma membrane |
| *RubisCO* | RubisCO | ↑5.3 | ↑5.3 | ↑5.3 | – | Carbon fixation | Chloroplast | Chloroplast |
| *HVCN1* | Voltage-gated $H^+$ channel | – | – | – | – | $H^+$ channel [b](Taylor *et al.*, 2011) | Plasma membrane (Taylor *et al.*, 2011) | Cytosol |
| *ATPVc'/c* | Vacuolar-type $H^+$ pump | ↑4.4 | ↑4.4 | ↑4.4 | – | Vacuolar-type ATP driven $H^+$ pump [b](Corstjens *et al.*, 2001) | Endomembrane system, possibly CV-associated membrane fraction (Corstjens *et al.*, 2001) | Vacuole |
| *PATP* | Plasma membrane type $H^+$ pump | ↑7.1 | ↑7.1 | ↑7.1 | – | 'PM'-type ATP driven $H^+$ pump | Plasma membrane | Plasma membrane |
| *CAX3* | $Ca^{2+}/H^+$ exchanger 3 | ↑4.4 | ↑4.4 | ↑4.4 | – | $Ca^{2+}/H^+$ exchanger – driven by a $H^+$ gradient | Endomembrane based on plant and yeast CAX proteins | Cytosol |
| *NhaA2* | $Na^+/H^+$ exchanger 2 | ↑4.9 | ↑4.9 | ↑4.9 | – | $Na^+/H^+$ exchanger – maintains cellular pH and membrane potential | – | Nucleus, cytosol |
| *LCIX* | Low $CO_2$ induced gene | ↑189.3 | ↑189.3 | ↑189.3 | – | Putative low $CO_2$ induced gene found in *Chlamydomonas* | Chloroplast but no transmembrane regions | Nucleus |
| *AQP2* | Aquaporin 2 | – | – | – | – | $H_2O$-permeable channel. Some are $CO_2$ permeable. | – | Plasma membrane |
| *GPA* | Glutamic acid, proline, alanine rich protein | ↑11 | ↑11 | ↑11 | – | $Ca^{2+}$ binding protein [b] (Corstjens *et al.*, 1998) | Coccolith vesicle? | Nucleus |

Arrows indicate a significant up-regulation ($P < 0.05$) of the investigated genes at low $CO_2$ (< 10 μmol $kg^{-1}$), $HCO_3^-$ (< 1000 μmol $kg^{-1}$), and $CO_3^{2-}$ (< 50 μmol $kg^{-1}$), compared with the lowest measured expression at high dissolved inorganic carbon (DIC) (> *c.* 1000 μmol $kg^{-1}$). Numbers behind arrows denote the maximum fold change that has been observed. Shading indicates a consistent up-regulation with decreasing levels of the respective carbonate system parameter (see Fig. 4).

[a]No statistical evaluation was possible because some replicates were below the detection limit.

[b]Indicates partially characterized in coccolithophores.

**Table 2** Presence or absence of *Emiliania huxleyi* coccoliths from SEM investigations

Table showing SEM analysis of individual replicates of treatments where particulate inorganic carbon (PIC) production was < 0.5 pg per cell $d^{-1}$. Note that coccoliths were found in all treatments and replicates not listed in this table.

[a]Cell concentrations were higher in this replicate at the end of the experiment (76 000 compared with 36 000 cell $ml^{-1}$ in first replicate). This caused a stronger decrease in [$HCO_3^-$] and [$H^+$].

| Experiment | $HCO_3^-$ (µmol $kg^{-1}$) | $H^+$ (nmol $kg^{-1}$) | Coccoliths found? |
|---|---|---|---|
| Constant $pH_f = 7.74$ | 200 | 18.2 | No |
| | 160 | 18.2 | No |
| | 200 | 18.2 | No |
| | 300 | 17.8 | No |
| | 330 | 17.8 | No |
| | 320 | 17.8 | No |
| Constant $pH_f = 8.34$ | 170 | 4.8 | Yes |
| | 160 | 4.7 | Yes |
| | 170 | 4.7 | Yes |
| Constant $CO_2$ | 520 | 30.9 | No |
| | 510 | 26.3 | No |
| | 490 | 22.9 | Yes[a] |

**Table 3** Assumptions within the conceptual model for inorganic carbon uptake in *Emiliania huxleyi*

| Assumption | Basis of assumption | Reference |
|---|---|---|
| Cellular organelle location and approximate relative sizes | Transmission electron micrographs | M. A. Gutowska *et al.* (unpublished) |
| $CO_2$ principal external inorganic carbon source for photosynthesis | $^{14}C$ labeling studies; membrane inlet mass spectrometry measurements | Sikes *et al.* (1980); Schulz *et al.* (2007) |
| Increasing $HCO_3^-$ over $CO_2$ usage for photosynthesis at low $CO_2$ | Membrane inlet mass spectrometry identifies increasing $HCO_3^-$ : $CO_2$ uptake ratio for cells acclimated to low-$CO_2$ conditions; up-regulation of AEL1 at low $CO_2$ | Rost *et al.* (2003); this study |
| $HCO_3^-$ pool and dual function of AEL1 in calcification and carbon-concentrating mechanism (CCM) | AEL1 previously shown to have a role in calcification; up-regulation at low dissolved inorganic carbon (DIC) | Mackinder *et al.* (2011); this study |
| Up-regulation of carbonic anhydrases (CAs) at low DIC | Three out of five investigated CAs showed an up-regulation in expression at low DIC | This study |
| Location of δCA at plasma membrane | Presence of a putative membrane anchor; localization of a dinoflagellate δCA to the plasma membrane; strong up-regulation at low $CO_2$ has also been demonstrated in TWCA1, a δCA from *Thalassiosira weissflogii*; up-regulation at low DIC | Soto *et al.* (2006); Lapointe *et al.* (2008); McGinn & Morel (2008); this study |
| Up-regulation of extracellular CA at low DIC | Increased extracellular CA activity at low DIC/high pH; up-regulation of δCA at low DIC | Nimer *et al.* (1997); this study |
| Localization of βCA to the chloroplast | Two βCAs from diatoms have been shown to localize to the chloroplast – specifically the pyrenoid; CA activity in the stroma chloroplast fraction of the coccolithophore *Pleurochrysis* sp. | Kitao *et al.* (2008) and Tachibana *et al.* (2011); Quiroga & González (1993) |
| Probable absence of cytosolic CA | Cytosolic acidification at high $HCO_3^-$ – presence of CA would result in rapid buffering; expression of a human CA in the cytoplasm of cyanobacteria resulted in a high $CO_2$-requiring phenotype; cytosolic CA would increase cytosolic $CO_2$, leading to increased leakage at low external $CO_2$ | Suffrian *et al.* (2011); Price & Badger (1989); this study |
| Switching off of calcification at low DIC to increase DIC availability for photosynthesis | The decrease in calcification before a reduction in particulate organic carbon (POC) and growth rates. The complete termination of calcification at low DIC and $pH_f$ | This study |
| $HCO_3^-$ is the principal substrate for calcification | Previous $^{14}C$ labeling studies; strong correlation of calcification with $HCO_3^-$ concentration | Sikes *et al.* (1980) and Nimer *et al.* (1997); Buitenhuis *et al.* (1999) and this study |
| The use of pH gradients within the CCM | Up-regulation of putative $H^+$ transporters at low DIC | Raven (1997); this study |
| Increase in RubisCO | Up-regulation of RubisCO to compensate for its decrease in efficiency as a result of an increased oxygenase : carboxylase ratio at low $CO_2$ | This study |

## References


Bach LT, Bauke C, Meier KJS, Riebesell U, Schulz KG. 2012. Influence of changing carbonate chemistry on morphology and weight of coccoliths formed by *Emiliania huxleyi*. Biogeosciences 9: 3449–3463.

Bach LT, Riebesell U, Schulz KG. 2011. Distinguishing between the effects of ocean acidification and ocean carbonation in the coccolithophore *Emiliania huxleyi*. Limnology and Oceanography 56: 2040–2050.

Badger M. 2003. The roles of carbonic anhydrases in photosynthetic $CO_2$ concentrating mechanisms. Photosynthesis Research 77: 83–94.

Bown PR, Lees JA, Young JR. 2004. Calcareous nannoplankton evolution and diversity through time. In: Thierstein HR, Young JR, eds. Coccolithophores – from molecular processes to global impact. Berlin, Germany: Springer Verlag, 481–505.

Brueggeman AJ, Gangadharaiah DS, Cserhati MF, Casero D, Weeks DP, Ladunga I. 2012. Activation of the carbon concentrating mechanism by $CO_2$ deprivation coincides with massive transcriptional restructuring in *Chlamydomonas reinhardtii*. Plant Cell 24: 1860–1875.

Buitenhuis E, de Baar H, Veldhuis M. 1999. Photosynthesis and calcification by *Emiliania huxleyi* (Prymnesiophyceae) as a function of inorganic carbon species. Journal of Phycology 35: 949–959.

Caldeira K, Wickett ME. 2003. Anthropogenic carbon and ocean pH. Nature 425: 365.

Corstjens P, Araki Y, Gonz alez EL. 2001. A coccolithophorid calcifying vesicle with a vacuolar-type ATPase proton pump: cloning and immunolocalisation of the V0 subunit c1. Journal of Phycology 37: 71–78.

Corstjens P, Van Der Kooij A, Linschooten C, Brouwers GJ, Westbroek P, de Vrind de Jong E. 1998. GPA, a calcium–binding protein in the coccolithophorid *Emiliania huxleyi* (Prymnesiophyceae). Journal of Phycology 34: 622–630.

von Dassow P, Ogata H, Probert I, Wincker P, Da Silva C, Audic S, Claverie JM, de Vargas C. 2009. Transcriptome analysis of functional differentiation between haploid and diploid cells of *Emiliania huxleyi*, a globally significant photosynthetic calcifying cell. Genome Biology 10: R114.

Dickson AG, Afghan JD, Anderson GC. 2003. Reference materials for oceanic $CO_2$ analysis: a method for the certification of total alkalinity. Marine Chemistry 80: 185–197.

Falkowski PG, Raven J. 2007. Aquatic photosynthesis. Princeton, NJ, USA: Princeton University Press.

Fernandez E, Balch WM, Maranon E, Holligan PM. 1994. High rates of lipid biosynthesis in cultured, mesocosm and coastal populations of the coccolithophore *Emiliania huxleyi*. Marine Ecology Progress Series 22: 13–22.

Field CB, Behrenfeld MJ, Randerson JT, Falkowski P. 1998. Primary production of the biosphere: integrating terrestrial and oceanic components. Science 281: 237–240.

Giordano M, Beardall J, Raven JA. 2005. $CO_2$ concentrating mechanisms in algae: mechanisms, environmental modulation, and evolution. Annual Review of Plant Biology 56: 99–131.

Guillard R, Ryther J. 1962. Studies of marine planktonic diatoms. I. Cyclotella nana Hustedt, and Detonula confervacea (cleve) Gran. Canadian Journal of Microbiology 8: 229–239.

Hansen HP, Koroleff F. 1999. Determination of nutrients. In: Grasshoff K, Kremling K, Ehrhardt M, eds. Methods of seawater analysis, 3rd edn. Weinheim, Germany: Wiley-VCH Verlag GmbH, 159–228.

Harada H, Nakatsuma D, Ishida M, Matsuda Y. 2005. Regulation of the expression of intracellular beta-carbonic anhydrase in response to $CO_2$ and light in the marine diatom *Phaeodactylum tricornutum*. Plant Physiology 139: 1041–1050.

Herfort L, Loste E, Meldrum F, Thake B. 2004. Structural and physiological effects of calcium and magnesium in *Emiliania huxleyi* (Lohmann) Hay and Mohler. Journal of Structural Biology 148: 307–314.

Herfort L, Thake B, Roberts J. 2002. Acquisition and use of bicarbonate by *Emiliania huxleyi*. New Phytologist 156: 427–436.

Horton P, Park K-J, Obayashi T, Fujita N, Harada H, Adams-Collier CJ, Nakai K. 2007. WoLF PSORT: protein localization predictor. Nucleic Acids Research 35: W585–W587.

Johnston AM, Raven JA. 1996. Inorganic carbon accumulation by the marine diatom *Phaeodactylum tricornutum*. European Journal of Phycology 31: 285– 290.

Kester DR, Duedall IW, Connors DN, Pytkowicz RM. 1967. Preparation of artificial seawater. Limnology and Oceanography 12: 176–179.

Kitao Y, Harada H, Matsuda Y. 2008. Localization and targeting mechanisms of two chloroplastic beta-carbonic anhydrases in the marine diatom *Phaeodactylum tricornutum*. Physiologia Plantarum 133: 68–77.

Krug SA, Schulz KG, Riebesell U. 2011. Effects of changes in carbonate chemistry speciation on Coccolithus braarudii: a discussion of coccolithophorid sensitivities. Biogeosciences 8: 771–777.

Langer G, Geisen M, Baumann K-H, Kl€as J, Riebesell U, Thoms S, Young JR. 2006. Species-specific responses of calcifying algae to changing seawater carbonate chemistry. Geochemistry Geophysics Geosystems 7: Q09006.

Langer G, Nehrke G, Probert I, Ly J, Ziveri P. 2009. Strain-specific responses of *Emiliania huxleyi* to changing seawater carbonate chemistry. Biogeosciences 6: 4361–4383.

Lapointe M, MacKenzie TDB, Morse D. 2008. An external d-carbonic anhydrase in a free-living marine dinoflagellate may circumvent diffusion limited carbon acquisition. Plant Physiology 147: 1427–1436.

LaRoche J, Rost B, Engel A. 2010. Bioassay, batch culture and chemostat experimentation. In: Riebesell U, Fabry V, Hansson L, Gattuso JP, eds. Guide for best practices for ocean acidification research and data reporting: Publications Office of the European Union, 81–94.

Leonardos N, Read B, Thake B, Young JR. 2009. No mechanistic dependence of photosynthesis on calcification in the coccolithophorid *Emiliania huxleyi* (Haptophyta). Journal of Phycology 45: 1046–1051.

Lewis E, Wallace DWR. 1998. Program developed for $CO_2$ systems calculations. Oak Ridge, TN, USA: ORNL/CDIAC-105 Carbon Dioxide Information Analysis Centre, Oak Ridge National Laboratory, US Department of Energy.

Mackinder L, Wheeler G, Schroeder D, von Dassow P, Riebesell U, Brownlee C. 2011. Expression of biomineralization-related ion transport genes in *Emiliania huxleyi*. Environmental Microbiology 13: 3250–3265.

McGinn PJ, Morel FM. 2008. Expression and regulation of carbonic anhydrases in the marine diatom Thalassiosira pseudonana and in natural phytoplankton assemblages from Great Bay, New Jersey. Physiologia Plantarum 133: 78–91.

Miura K, Yamano T, Yoshioka S, Kohinata T, Inoue Y, Taniguchi F, Asamizu E, Nakamura Y, Tabata S, Yamato KT, et al. 2004. Expression Profiling-Based Identification of $CO_2$-responsive genes regulated by CCM1 controlling a carbon-concentrating mechanism in *Chlamydomonas reinhardtii*. Plant Physiology 135: 1595–1607.

Moore TS, Dowell MD, Franz BA. 2012. Detection of coccolithophore blooms in ocean color satellite imagery: a generalized approach for use with multiple sensors. Remote Sensing of Environment 117: 249–263.

Moroney J, Ma Y, Frey W, Fusilier K, Pham T, Simms T, DiMario R, Yang J, Mukherjee B. 2011. The carbonic anhydrase isoforms of *Chlamydomonas reinhardtii*: intracellular location, expression, and physiological roles. Photosynthesis Research 109: 133–149.

Nakajima K, Tanaka A, Matsuda Y. 2013. SLC4 family transporters in a marine diatom directly pump bicarbonate from seawater. Proceedings of the National Academy of Sciences, USA 110: 1767–1772.

Nimer NA, IglesiasRodriguez MD, Merrett MJ. 1997. Bicarbonate utilization by marine phytoplankton species. Journal of Phycology 33: 625–631.

Nimer NA, Merrett MJ. 1992. Calcification and utilization of inorganic carbon by the coccolithophorid *Emiliania huxleyi* Lohmann. New Phytologist 121:173–177.

Paasche E. 1964. A tracer study of the inorganic carbon uptake during coccolith formation and photosynthesis in the coccolithophorid *Coccolithus huxleyi*. Physiologia Plantarum Supplementum 3: 1–82.

Paasche E. 2001. A review of the coccolithophorid *Emiliania huxleyi* (Prymnesiophyceae), with particular reference to growth, coccolith formation, and calcification-photosynthesis interactions. Phycologia 40: 503–529.

Poulton AJ, Adey TR, Balch WM, Holligan PM. 2007. Relating coccolithophore calcification rates to phytoplankton community dynamics: regional differences and implications for carbon export. Deep Sea Research Part II 54: 538–557.

Price GD, Badger MR. 1989. Expression of human carbonic anhydrase in the cyanobacterium Synecoccus PCC 7942 creates a high $CO_2$-requiring phenotype. Plant Physiology 91: 505–513.

Purdie DA, Finch MS. 1994. Impact of a coccolithophorid bloom on dissolved carbon dioxide in sea water enclosures in a Norwegian fjord. Sarsia 79: 379–387.

Quiroga O, Gonz alez EL. 1993. Carbonic anhydrase in the chloroplast of a coccolithophorid (Prymnesiophyceae). Journal of Phycology 29: 321–324.

Raven J. 1997. Putting the C in phycology. European Journal of Phycology 32: 319–333.

Raven JA, Giordano M. 2009. Biomineralization by photosynthetic organisms: evidence of coevolution of the organisms and their environment? Geobiology 7: 140–154.

Reinfelder JR. 2011. Carbon concentrating mechanisms in eukaryotic marine phytoplankton. Annual Review of Marine Science 3: 291–315.

Ridgwell A. 2005. A Mid Mesozoic revolution in the regulation of ocean chemistry. Marine Geology 217: 339–357.

Ridgwell A, Schmidt DN, Turley C, Brownlee C, Maldonado MT, Tortell P, Young JR. 2009. From laboratory manipulations to earth system models: predicting pelagic calcification and its consequences. Biogeosciences Discussions 6: 3455–3480.

Riebesell U, Tortell PD. 2011. Effects of ocean acidification on pelagic organisms and ecosystems. In: Gattuso JP, Hansson L, eds. Ocean acidification. Oxford, UK: Oxford University Press, 99–121.

Riebesell U, Zondervan I, Rost B, Tortell PD, Zeebe RE, Morel FMM. 2000. Reduced calcification of marine plankton in response to increased atmospheric $CO_2$. Nature 407: 364–367.

Rokitta SD, Rost B. 2012. Effects of $CO_2$ and their modulation by light in the life-cycle stages of the coccolithophore *Emiliania huxleyi*. Limnology & Oceanography 57: 607–618.

Rost B, Riebesell U, Burkhardt S, S€ultemeyer D. 2003. Carbon acquisition of bloom-forming marine phytoplankton. Limnology and Oceanography 48: 55–67.

Rost B, Riebesell U, S€ultemeyer D. 2006. Carbon acquisition of marine phytoplankton: effect of photoperiod length. Limnology and Oceanography 51: 12–20.

Roy RN, Roy LN, Vogel KM, Porter-Moore C, Pearson T, Good CE, Millero FJ, Campbell DM. 1993. The dissociation constants of carbonic acid in seawater at salinities 5 to 45 and temperatures 0 to 45°C. Marine Chemistry 44: 249–267.

Sarmiento J, Gruber N. 2006. Ocean biogeochemical dynamics. Princeton, NJ, USA: Princeton University Press.

Schulz KG, Rost B, Burkhardt S, Riebesell U, Thoms S, Wolf-Gladrow DA. 2007. The effect of iron availability on the regulation of inorganic carbon acquisition in the coccolithophore *Emiliania huxleyi* and the significance of cellular compartmentation for stable carbon isotope fractionation. Geochimica et Cosmochimica Acta 71: 5301–5312.

Sekino K, Shiraiwa Y. 1994. Accumulation and utilization of dissolved inorganic carbon by a marine unicellular coccolithophorid, *Emiliania huxleyi*. Plant and Cell Physiology 35: 353–361.

Sikes CS, Roer RD, Wilbur KM. 1980. Photosynthesis and coccolith formation – inorganic carbon-sources and net inorganic reaction of deposition. Limnology and Oceanography 25: 248–261.

Soto AR, Zheng H, Shoemaker D, Rodriguez J, Read BA, Wahlund TM. 2006. Identification and preliminary characterization of two cDNAs encoding unique carbonic anhydrases from the marine alga *Emiliania huxleyi*. Applied and Environmental Microbiology 72: 5500–5511.

Spalding MH. 2008. Microalgal carbon-dioxide-concentrating mechanisms: *chlamydomonas* inorganic carbon transporters. Journal of Experimental Botany 59: 1463–1473.

Stoll MHC, Bakker K, Nobbe GH, Haese RR. 2001. Continuous-flow analysis of dissolved inorganic carbon content in seawater. Analytical Chemistry 73: 4111–4116.

Suffrian K, Schulz KG, Gutowska MA, Riebesell U, Bleich M. 2011. Cellular pH measurements in *Emiliania huxleyi* reveal pronounced membrane proton permeability. New Phytologist 190: 595–608.

Tachibana M, Allen A, Kikutani S, Endo Y, Bowler C, Matsuda Y. 2011. Localization of putative carbonic anhydrases in two marine diatoms, *Phaeodactylum tricornutum* and *Thalassiosira pseudonana*. Photosynthesis Research 109: 205–221.

Taylor AR, Chrachri A, Wheeler G, Goddard H, Brownlee C. 2011. A voltage-gated $H^+$ channel underlying pH homeostasis in calcifying coccolithophores. Plos Biology 9: e1001085.

Thierstein HR, Geitzenauer KR, Molfino B, Shackleton NJ. 1977. Global synchroneity of late Quaternary coccolith datum levels validation by oxygen isotopes. Geology 5: 400–404.

Trimborn S, Langer G, Rost B. 2007. Effect of varying calcium concentrations and light intensities on calcification and photosynthesis in *Emiliania huxleyi*. Limnology and Oceanography 52: 2285–2293.

Trimborn S, Wolf-Gladrow D, Richter K-U, Rost B. 2009. The effect of $pCO_2$ on carbon acquisition and intracellular assimilation in four marine diatoms. Journal of Experimental Marine Biology and Ecology 376: 26–36.

Vandesompele J, De Preter K, Pattyn F, Poppe B, Van Roy N, De Paepe A, Speleman F. 2002. Accurate normalization of real-time quantitative RT-PCR data by geometric averaging of multiple internal control genes. Genome Biology 3: research0034.0031–research0034.0011

Wang Y, Spalding MH. 2006. An inorganic carbon transport system responsible for acclimation specific to air levels of $CO_2$ in *Chlamydomonas reinhardtii*. Proceedings of the National Academy of Sciences, USA 103: 10110–10115.

Wolf-Gladrow DA, Riebesell U, Burkhardt S, Bijma J. 1999. Direct effects of $CO_2$ concentration on growth and isotopic composition of marine plankton. Tellus Series B Chemical and Physical Meterology 51: 461–476.

Zeebe RE, Wolf-Gladrow D. 2001. $CO_2$ in seawater: equilibrium, kinetics, isotopes. Amsterdam, the Netherlands: Elsevier.